Chapter 4

Storm Track Dynamics

Kyle L. Swanson

4.1. Introduction

It has long been appreciated that mobile, $O(1000\,\text{km})$ spatial scale high and low pressure systems comprise much of the day-to-day weather variability in the midlatitudes. Coupled with the central role of these systems in the general circulation via their transports of sensible heat, momentum, and moisture, it is natural that the geographic organization of these transients is an important topic if one is to understand the climate of the Earth's atmosphere. Areas of preferred transient or storm (cyclone) activity are referred to as storm tracks.

Historically, there have been two basic approaches to diagnosing storm tracks (see Hoskins and Hodges [2002] for a review). The more traditional approach identifies individual weather systems, tracks their position as a function of time, and produces statistics for their distributions, e.g., track densities, storm life spans, etc. An alternative approach determines statistics at a set of grid points in analyzed atmospheric fields, usually in a frequency band associated with what are considered to be synoptic time scales (e.g., Blackmon 1976; Blackmon et al. 1977). The latter bandpass filtering approach has the advantage that it can be carried out at all levels of the atmosphere, providing a three-dimensional picture of storm tracks. Further, it is more consistent with the view that storm tracks are statistical features of the climate, in the same manner, for example, that the global mean temperature distribution is a statistical feature of the climate. This approach provides a definition of storm tracks as geographically localized maxima in bandpass transient variance. An example of a storm track structure that emerges from such an analysis is shown in Fig. 4.1 (top), where the storm tracks are marked in the bandpass standard deviation of the 250-hPa geopotential height field by enhanced variability off the east coasts of Asia and North America.

The structure of the bandpass standard deviation field in Fig. 4.1 (top) suggests the primary question that has arisen time and time again in the study of storm track dynamics, namely what features of the background time-mean flow determine the

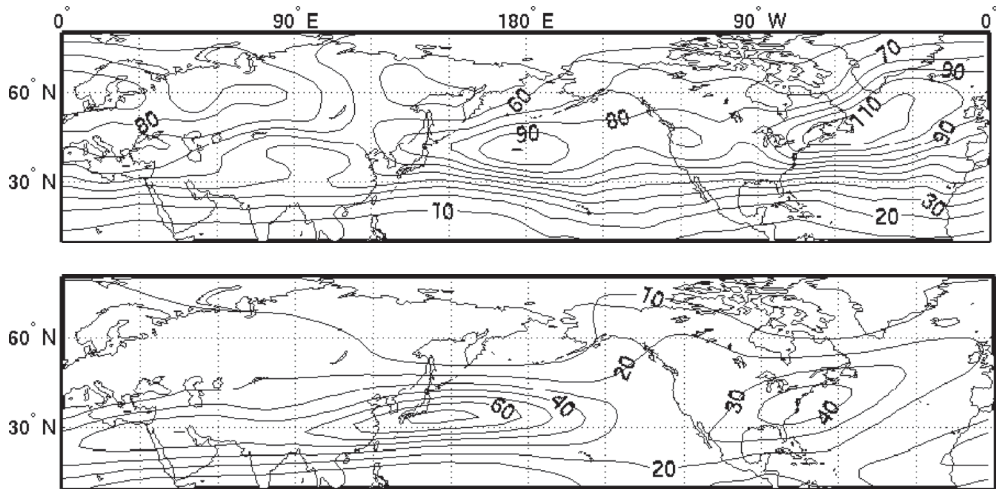

FIGURE 4.1. Top: 250-hPa geopotential height bandpass (3–10 day) standard deviation for January/February (m). Bottom: 250-hPa mean zonal winds for January/February ($\mathrm{m\,s^{-1}}$).

magnitude and degree of zonal localization of storm tracks? Since the synoptic transients that compose the storm tracks feed off of the available potential energy stored in the meridional pole-to-equator temperature gradient, it is natural to associate storm tracks with localized regions of large meridional temperature gradients, or baroclinic zones. A suitable measure of that baroclinicity is given by the Eady growth-rate maximum

$$\sigma_{\mathrm{BI}} = 0.31\, f |\partial \mathbf{v}/\partial z| N^{-1}, \qquad [4.1]$$

where f is the Coriolis parameter, N the Brunt-Väisälä frequency, and $\mathbf{v}$ the time-mean wind field. Lindzen and Farrell (1980) show that this formula provides an accurate estimate of growth rate in a range of baroclinic instability problems, suggesting an intimate link between the vertical shear and disturbance growth. Figure 4.1 (bottom) shows that during the Northern Hemisphere winter the baroclinic zones, marked by the climatological jet streams in the upper troposphere via thermal wind balance, are located off the east coast of the Asian and North American continents. The storm tracks are located just downstream (eastward) from these baroclinic zones, hinting at spatio-temporal amplification of synoptic eddies as they travel eastward through these zones. However, this observation raises more questions than it answers: What determines how far downstream of the region of maximum baroclinicity the maximum transient variance occurs? What is the physical mechanism responsible for terminating the storm tracks? Is it consistent to view the storm tracks as being determined solely by the properties of the background flow?

The importance of answering these questions is highlighted by the fact that storm tracks exhibit stunning modes of variability on intra-annual, interannual, and decadal time scales, as discussed by Chang et al. (2002). For example, Fig. 4.2 shows the 250-hPa

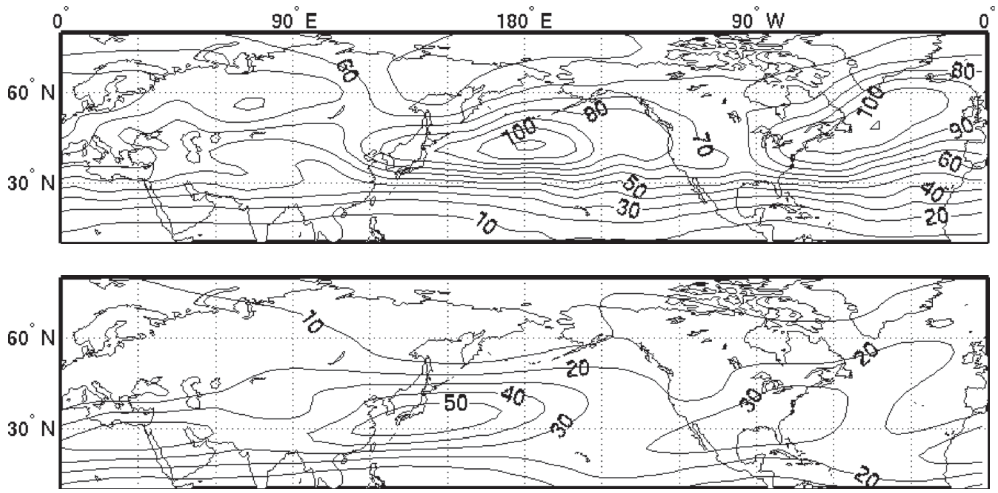

FIGURE 4.2. Top: 250-hPa geopotential height bandpass (3–10 day) standard deviation for March/April (m). Bottom: 250-hPa mean zonal winds for March/April ($m\,s^{-1}$).

geopotential height bandpass standard deviation and mean zonal wind for the months of March/April. Comparison between this figure and Fig. 4.1 reveals that in spite of substantially weaker mean zonal winds (and hence weaker baroclinicity) over the Pacific during March/April, transient variance is actually larger over the Pacific than it is during January/February. This so-called "midwinter minimum" in Pacific storm track activity was first noted by Nakamura (1992); a concise theoretical explanation has remained elusive. Given this and other types of observed storm track variability, it is presumed that changes in storm tracks will play a major role in shaping future climate change (Hall et al. 1994).

Significant progress has been made over the past three decades in explaining how observed storm tracks function and diagnosing modes of storm track variability. A range of idealized models have been used to explore different modes of observed storm track variability with success. However, intercomparison between various theoretical and idealized storm track models and observed structures remains difficult. This leaves aside the difficult questions posed by the paleoclimate record, where evidence is consistent with multiple modes of storm track variability, variability not captured by the current generation of climate models (see Broecker [1997] and chapter 12 in this volume).

Ideally, a theory of storm track dynamics would provide straightforward answers to the set of storm track questions raised above. However, the issues raised when considering observed storm track dynamics are by nature difficult, and it is not clear that direct comparison of theoretical ideas with observations is the best manner in which to proceed. Observed storm track dynamics have a number of complicating factors that may well be important, in particular the role of moisture, that are missing from current theoretical models. Given this state of affairs, in this chapter a different approach is followed to the dynamics of storm tracks, namely the comparison of theoretical ideas

and simple models against models of comparable complexity. As discussed by Held and Hoskins (1985), such an approach provides unambiguous answers to the underlying dynamical issues addressed, allowing one to build experience in treating dynamical issues that ultimately may be extended to the observational arena.

4.2. Overview

Since storm tracks consist of a statistically steady composite of synoptic eddies at various points in their life cycles, the synoptic eddy life cycle is a natural starting point to understand storm track dynamics. As outlined in studies such as Simmons and Hoskins (1980), the synoptic eddy life cycle consists of a baroclinic growth stage, followed by ultimate saturation and decay primarily by barotropic processes. Baroclinic growth is marked by cyclogenesis at the surface, with the eddy growth at upper levels following, with saturation occurring first at the surface followed by the upper levels. From the perspective of the Eliassen-Palm flux (Andrews et al. 1987; see also chapter 5 in this volume), this is consistent with downgradient heat fluxes during the early part of the eddy life cycle, followed by radiation of eddy activity onto the flanks of the jet via meridional momentum fluxes, where dissipation occurs by Rossby wave breaking-like processes (Killworth and McIntyre 1985).

Of course, the synoptic eddy life cycle above describes disturbance growth and decay as a function of time. The most basic idea of storm track structure equates this disturbance life cycle in time with a disturbance life cycle in space within the storm track. Disturbances are introduced at the upstream end of the storm track, and develop in space and time as they extract energy from the enhanced baroclinicity of the background flow. The downstream end of the storm track is then marked by the decay stage of the synoptic eddy life cycle. An estimate of the storm track length then is simply the time span of the synoptic eddy life cycle divided by the phase speed of the individual eddies.

While this picture is appealing in that it retains the synoptic eddy life cycle as the distinguishing element, it has a number of faults. First, the estimate of storm track length described above is about a factor of two too small compared to observed Northern Hemisphere winter storm tracks. Nonlinear life cycle experiments give disturbance growth to decay stages of about 5 days (Simmons and Hoskins 1980), which when coupled with a 7–8 $\mathrm{m\,s^{-1}}$ phase speed (Chang 1993) suggests a storm track length of roughly 3000 km, whereas the observed storm tracks of Figs. 4.1 and 4.2 are more like 8–10,000 km in length. In addition, statistical decomposition reveals that there is not really a bottom-trapped, baroclinic growth phase for the transients (Lim and Wallace 1991; Chang 1993). This is most readily shown by examining regressions of storm track transients, an example of which is shown in Fig. 4.3. This regression of meridional wind along the latitude circle 40°N against the meridional wind at the point (175°E, 300 hPa) provides a picture of the characteristic scale of transients, as well as of the

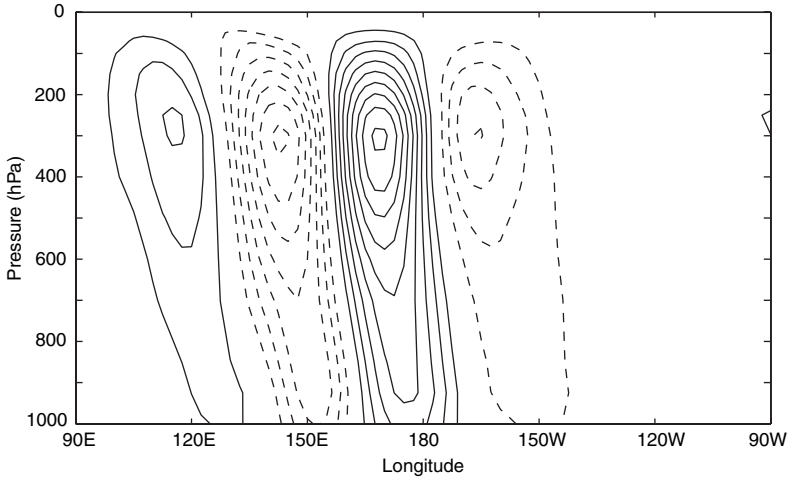

FIGURE 4.3. Regression of meridional velocity along 40° N against the point at (175° E, 300 hPa). The contour interval is 2 m s^{-1}, with negative contours dashed.

wavy structure of disturbances. Notably, there is little difference between disturbance structures upstream or downstream of the regression point. Disturbances are somewhat tilted more strongly against the shear upstream of the regression point, but there is not a clear counterpart to the surface cyclogenesis found in traditional life cycle experiments of the type described by Simmons and Hoskins (1980).

A more fundamental difference between transients in storm tracks and traditional life cycles is the sense of group propagation within storm tracks, which suggests that the phase speed (the speed of individual cyclones) is not the relevant speed for storm track structure. Figure 4.4 shows the correlation of the meridional wind field against the meridional wind at a point in the center of the Pacific storm track, along with the analogous fields that lag and lead that point by one day. There is an obvious sense of group propagation—disturbances upstream of the base disturbance are stronger in the day−1 correlation, while those downstream are stronger in the day +1 correlation. As shown by Chang (1993), this group speed is more characteristic of the upper-tropospheric background flow, roughly 40 m s^{-1}, in contrast to the speed of individual cyclones, which resembles the flow at the steering level of about 700 hPa, roughly 7–8 m s^{-1}.

The picture that emerges from this analysis is one of modulated wave packets of synoptic disturbances, exemplified by the nonlinear baroclinic wave packets that have been noted in both the Northern and Southern Hemispheres and in simple models (Lee and Held 1993; Chang 1993, 1999, 2000, 2001). The dominance of the group propagation dynamic in the regression analysis indicates that the manner in which these packets of eddies interact with streamwise variations in the background flow ultimately determines storm track structure. The key issue then boils down to how these packets amplify and decay as they propagate through a streamwise varying background flow.

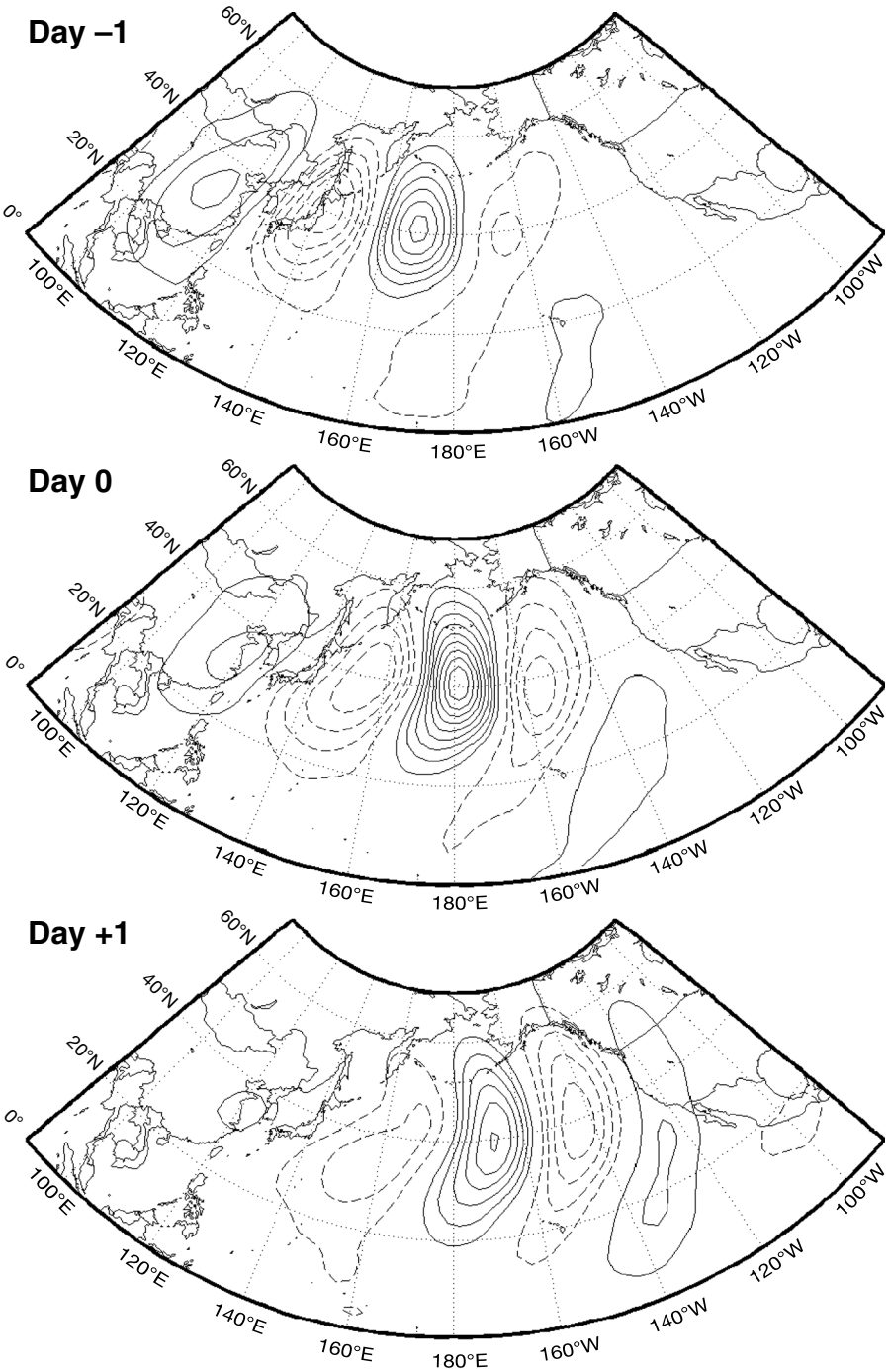

FIGURE 4.4. Correlation of meridional velocity on the 300 hPa surface against the point (40° N, 175° E). In the top panel, the correlated fields lag that point by 1 day, in the middle they are simultaneous, and in the bottom panel that point leads the fields by 1 day. The contour interval is 0.1, with negative contours dashed and the zero contour omitted.

The potent nature of the group dynamic within these packets is illustrated by Chang and Orlanski (1993), who show that there is no intrinsic downstream limit to storm tracks—once the transients are in place, the group dynamic allows the track to extend an indefinite distance downstream. However, sufficient barotropic deformation in the background flow can act to localize storm tracks (Lee 1995). This deformation is visible in the tendency of disturbances to become stretched in the meridional direction and compressed in the zonal direction in the eastern Pacific as shown in Fig. 4.4. This stretching marks the barotropic transfer of disturbance energy into the background flow (Cai and Mak 1990). However, this process need not be irreversible, and may simply mark an elastic interaction of the propagating wave packet with the streamwise varying background flow (Swanson et al. 1997). Other processes, such as storm track tilt (Frisius et al. 1998), surface friction, and the stability of the near-surface atmospheric layers no doubt also play a part in determining the details of storm track structure.

This analysis suggests that a minimal storm track theory must explain the storm track length in relation to an imposed background flow, along with the associated disturbance fluxes of heat and momentum, while retaining the sense of group dynamics. It is difficult to formulate such a theory for a model containing complete physical processes (moisture, etc.), let alone in the observed setting. In general, theoretical approaches are most valuable when they are applied in a setting in which the assumptions underlying the theory are satisfied. In this way, one develops experience in judging the strengths and weaknesses of a given theoretical approach in a clean setting, which provides the comfort that if the theory is adequate in such a setting, it may scale to provide explanations of behaviors found in more complete models or the observations. This is how the problem of storm track dynamics is approached here, first examining an intermediate model that possesses realistic storm track dynamics, followed by a comparison of the various theories of storm track behavior against model behavior.

4.3. Storm Track Variability: A Case Example

4.3.1. Dynamical Setting

Consider the nondimensional equations describing the quasigeostrophic flow of a two-layer fluid on the beta plane. Let $\lambda = (g\delta\rho\, D/\rho_0 f_0^2)^{1/2}$ be the deformation radius based upon the total fluid depth D, where ρ_0 is the average fluid density and $\delta\rho$ the density difference between the two layers, and let U be an as yet unspecified velocity scale. If we nondimensionalize lengths by λ, velocities by U, and times by λ/U, the governing dynamical equation can be written

$$\partial_t q_n + J(\psi_n, q_n) = S_n, \qquad [4.2]$$

where $n = 1$ corresponds to the upper layer and $n = 2$ corresponds to the lower layer. Here, ψ_n is the streamfunction and q_n is the potential vorticity, which is given by

$$q_n = \nabla^2 \psi_n - (-1)^n(\psi_2 - \psi_1)/2 + \beta y. \qquad [4.3]$$

In (4.3), $\beta = \beta^* \lambda^2 / U$ is a nondimensional parameter, where β^* is the dimensional planetary vorticity gradient. The source/sink term S_n generally includes radiative relaxation of the temperature $\theta = (\psi_1 - \psi_2)/2$ to some radiative equilibrium profile θ_{eq} with some time scale τ_{rad}, and Ekman damping of the vorticity in the lower layer on a timescale τ_{ek}. The velocity scale U is chosen consistent with the maximal imposed zonal-mean radiative equilibrium shear Δ, leaving $\xi = \beta^{-1}$ as a measure of the supercriticality of the zonal-mean flow (cf. chapter 1 in this volume; the supercriticality measure in chapter 1 differs from that here by a factor 2).

To study storm track dynamics, it is necessary to introduce zonal asymmetry in some form. If we restrict our focus to the Northern Hemisphere winter, two physical mechanisms are of particular importance in forcing the observed asymmetry. First, there are substantial zonal variations in the baroclinicity, with strong baroclinic zones off the east coasts of Asia and North America, where warm oceanic currents abut cold wintertime continental interiors. These temperature contrasts at the surface are communicated into the interior of the atmosphere by longwave radiative energy transfer, along with latent and sensible heat fluxes in the turbulent boundary layer and convective processes, resulting in the effective damping of the depth-integrated atmospheric profile to a zonally varying temperature distribution. Also, there are the prominent stationary wave patterns forced by topography and zonally varying heating; see the review by Held et al. (2002).

To simplify the issue, for the cases examined herein we consider a zonal asymmetry in the planetary-scale flow forced by radiative relaxation to a zonally asymmetric temperature profile of the form

$$\theta_{eq} = \frac{1}{2}\Delta\sigma \tanh(y/\sigma)(1 - \gamma e^{-(y/5\sigma)^2} \cos 2\pi x/L), \qquad [4.4]$$

where L is the domain length, σ is the jet width, and Δ is the shear of the radiative equilibrium jet. Note that caution must be applied in interpreting the results of any model response to simplified forcing such as this—as detailed by Andrews (1984), forcing that interacts with disturbances complicates the dynamical interpretation of zonally asymmetric flows.

Suppose that the zonally averaged flow in each layer is U_n. In the absence of zonal asymmetry ($\gamma = 0$) and eddies, the flow will be zonal, U_2 will vanish, and

$$U_1 = U_{\text{eq}} = -2\frac{\partial \theta_{\text{eq}}}{\partial y} \equiv \Delta \text{sech}^2(y/\sigma). \qquad [4.5]$$

If we choose Δ as the velocity scale, a horizontally uniform vertical shear $U_1 - U_2 \equiv 1$ is baroclinically unstable by Phillips's criterion, in the absence of damping, if $\beta < 1/2$.

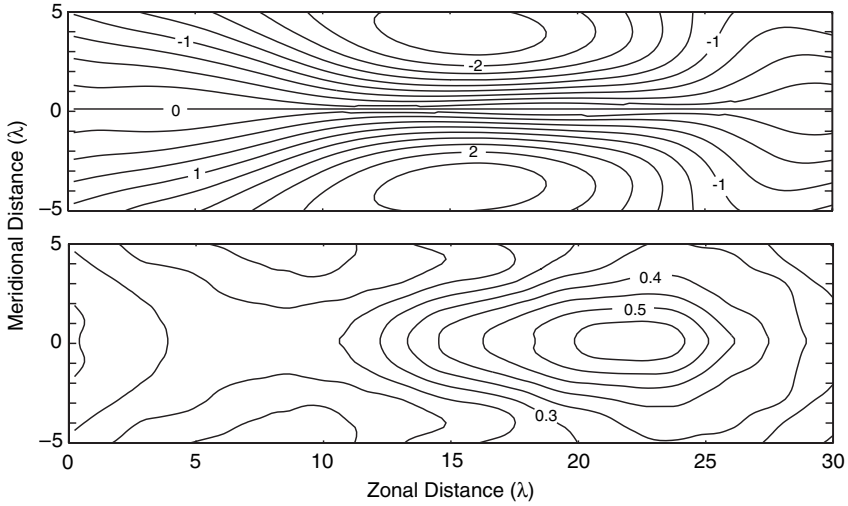

FIGURE 4.5. Top: Base case upper-layer time-mean streamfunction. Bottom: Base case high-pass (1–10 day) standard deviation of upper-layer streamfunction. Units are λU for both panels.

Given this situation, there are a number of parameters that in general will influence storm track structure and amplitude; the supercriticality $\xi = \beta^{-1}$, the zonal asymmetry γ, the jet width σ, and the thermal and mechanical damping parameters τ_{rad} and τ_{ek}. For reference, one nondimensional time unit is roughly one-half day for the values $\lambda = 800$ km and $U = 20\,\text{m}\,\text{s}^{-1}$. In general, we will speak in terms of dimensional quantities for ease of interpretation.

4.3.2. Base Case

Figure 4.5 shows the upper-layer time-mean streamfunction and bandpass streamfunction standard deviation for the moderately supercritical situation $\beta = 0.1$, where the jet width $\sigma = 1.5\lambda$ and the zonal asymmetry parameter $\gamma = 3.5$. The storm track system evolves in a wide channel with zonal length $L = 30\lambda$. The radiative and Ekman damping times are $\tau_{\text{rad}} = 30$ days and $\tau_{\text{ek}} = 5$ days, respectively, and the model is initialized from a state of rest perturbed by small amplitude vorticity disturbances in both layers. Since storm tracks are statistical creatures by nature, in principle one might expect the precise nature of this initial condition to be immaterial. This assumption shall be discussed further in section 4.6, but for the examples in the next two sections, the statistical steady state is independent of the initial conditions.

Certain aspects of observed storm tracks are well captured by this model. Localized storm tracks are found in both layers, with the upper-layer track displaced roughly λ downstream from the upper-layer jet maxima, and the standard deviation in the upper layer roughly twice that in the lower layer. The model's fluxes also resemble

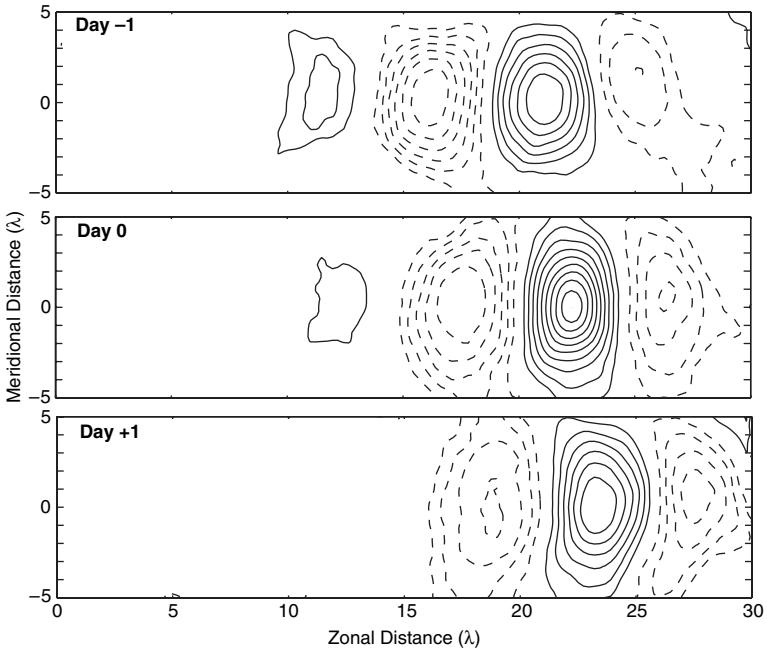

FIGURE 4.6. Correlation of meridional wind in the upper layer against the point 22λ at the channel center. In the top panel, the correlated fields lag that point by 1 day, in the middle they are simultaneous, and in the bottom panel that point leads the fields by 1 day. The contour interval is 0.1, with negative contours dashed and the zero contour omitted.

the observed, with the heat flux largest over the upstream end of the storm track and the momentum fluxes largest on the downstream end of the storm track on the flanks of the jet. The ability of this model to mimic observed storm track structures carries over to its spatio-temporal behavior. Figure 4.6 shows the one-point lagged correlations for a point located at the channel center at the zonal distance 22λ. As in the observed case, there is a distinct signature of group propagation different from phase propagation. This is marked by the larger magnitude correlations upstream of the base disturbance for the leading case (day $-$ 1), and downstream of the base disturbance for the lagging case (day $+$ 1). As in the observations, this group speed is more characteristic of the upper-layer flow, while the phase speed is similar to the lower-layer flow.

In the upper layer, the transients result in a downgradient flux of potential vorticity, particularly on the flanks of the jet. Such mixing is consistent with an acceleration of the flow along the jet axis, which itself is counteracted by dissipation of momentum in the lower-layer Ekman layer, resulting in mean westerlies in both layers. Geographically, this mixing is concentrated downstream of the baroclinic zone. Locally, the potential vorticity fluxes have substantial components both down the basic state potential vorticity gradient as well as along basic state potential vorticity contours, complicating the interpretation of the interaction of transients with the time-mean flow

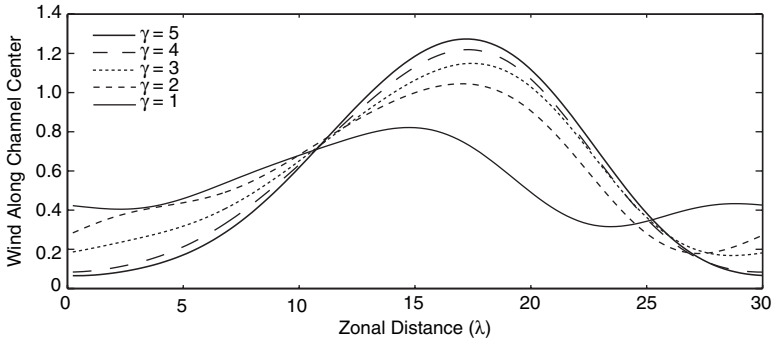

FIGURE 4.7. Time-mean zonal wind along the channel center for the perturbed storm track cases.

in comparison to the zonal-mean case. The issue of transient-mean flow interaction in storm tracks becomes involved rather quickly; Kushner and Held (1999) contains a discussion of these issues at an advanced level.

4.3.3. Storm Track Perturbations

A classic problem in storm track dynamics is the statistically steady response of a storm track to an imposed forcing to the basic state flow, such as heating due to an El Niño sea surface temperature anomaly. For the situation here, perhaps the simplest basic state perturbation involves adjusting the zonal asymmetry parameter γ. Other parameters, of course, are also of interest; Zurita-Gotor and Chang (2005) provide an in-depth examination of the response of a storm track to changes in the barotropic wind in a model similar to that here.

Figure 4.7 reveals that the response of the time-mean zonal wind component along the channel center to changes in γ is quite substantial. For the value $\gamma = 1$, the jet in the upper layer is nearly in phase with the radiative forcing, but increasing the asymmetry γ beyond this level results in a jet roughly 3λ downstream from the radiative forcing maximum, with the maximum jet speed increasing more or less consistently with γ. Corresponding weakening of the zonal flow away from the jet as γ is increased results in only small changes in the zonal-mean zonal flow as a function of γ. This contrast between the substantial local increases in jet strength (and hence baroclinicity) and the relatively benign global change in zonal-mean zonal wind is important to keep in mind when the discussion turns to the dynamics linearized around time-mean flows in section 4.4.

Figure 4.8 shows that the bandpass standard deviation associated with the variation in γ scales in a manner similar to that of the wind itself, increasing more where the time-mean zonal wind is large, with a weaker response where the time-mean zonal wind is small. This response is not surprising; since the lower-layer flow is small, the upper-layer time-mean zonal wind along the channel center provides a measure of the baroclinicity of the system, with stronger time-mean zonal winds associated with

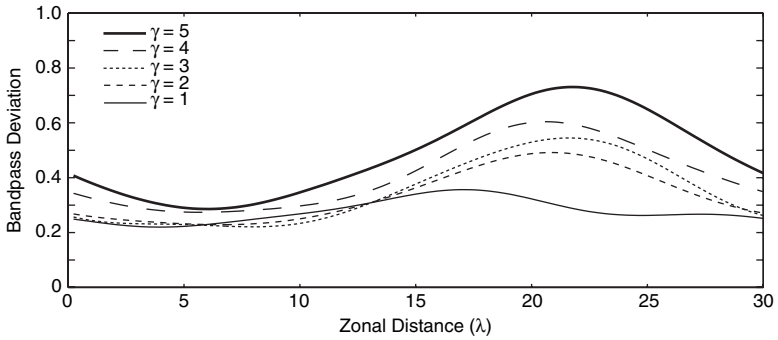

FIGURE 4.8. Bandpass standard deviation of upper-layer streamfunction along the channel center for the perturbed storm track cases as a function of γ.

higher baroclinicity. It is natural that disturbances should amplify more in response to this enhanced baroclinicity as they traverse the storm track. Additionally, this behavior highlights the importance of the zonal waveguide; where that waveguide is well formed, i.e., locations where the zonal flow is large, and upper-layer potential vorticity gradients are large, is where significant changes in transient variance occur.

This variation in bandpass standard deviation in response to changes in γ provides a reasonable set of test cases for storm track theories, which we explore in detail in the next section.

4.4. Linear Theories

Synoptic eddies and storm tracks are almost always discussed in relation to a background flow, whether that flow is steady, time mean, slowly evolving, or representative of some "instantaneous" weather regime. Such a separation of the flow into mean and eddy parts often presents conceptual difficulties, and also raises the issue of whether, and to what extent, the mean flow actually determines the eddy statistics or vice versa. However, in the context of storm track dynamics, it seems reasonable to inquire to what extent one can deduce storm track structure given an appropriate time-mean flow. This is the question addressed by mean field theories, of which linear theories are an important subset.

Insofar as one can successfully develop a linear theory linking storm tracks to the basic state flow, such a theory would be quite powerful. It is by now understood that changes in storm track structure force a substantial component of interannual stationary planetary wave activity (Lau and Holopainen 1984; Branstator 1992, 1995). A theory for storm track structural shifts could then be coupled with a stationary wave model, for example, providing a theory for the extratropical response to forced interannual variability.

Linear theories for storm tracks are linked to the initial-value problem of disturbance evolution and differ primarily over what time scales are important to the

overall storm track structures. Normal mode theory, with its emphasis on exponentially amplifying disturbances, assumes that disturbance structures in the long time limit are most important. In contrast, various stochastic theories either examine disturbance structures at a presupposed time, or add sufficient artificial dissipation to stabilize the linear system and, as such, effectively consider the time integral of the disturbance response. Let us consider how well these theories do at explaining the base and perturbed storm track structures from the nonlinear model simulations described above.

4.4.1. Normal Modes

Following the success in explaining certain aspects of synoptic eddy structure by examining linearly growing disturbances on zonally symmetric flows, as discussed by Pierrehumbert and Swanson (1995), it is reasonable to inquire whether examining the three-dimensional stability problem with a zonally varying flow provides insight into storm track structure. Upon substituting

$$\begin{aligned} \psi_n &= \overline{\psi}_n(x, y) + \psi'(x, y, t) \\ q_n &= \overline{q}_n(x, y) + q'(x, y, t) \end{aligned} \qquad [4.6]$$

and neglecting terms quadratic in the perturbation quantities, the linearized equations of motion are found to be

$$\partial_t q'_n + J(\overline{\psi}_n, q'_n) + J(\psi'_n, \overline{q}_n) = S'_n. \qquad [4.7]$$

In principle, one can solve this problem analytically or semi-analytically in the limit of slow streamwise variations in the imposed flow, following Pierrehumbert (1984). However, for more realistic models and flows, such a procedure becomes tedious. In such situations, one is left with solving the linear problem (4.7) directly for the zonally varying background flow.

For a specific first example, consider the linear response to the base-case time-mean flow shown in Fig. 4.5, neglecting (for the time being) forcing and dissipation by setting $S'_n = 0$. Integrating this condition forward for a sufficiently long time isolates a wavy normal mode, one phase of which is shown in Fig. 4.9. Consistent with Fredricksen (1983), this normal mode has structural characteristics similar to the nonlinear model's base-case highpass transient variability, and the scale of the waves themselves is similar to transient structures obtained from constructing point correlations in the evolving fully nonlinear flow, as shown in Fig. 4.6. In particular, it appears to capture the zonal structure of the variance, with peak variance between $x = 20\lambda$ and $x = 25\lambda$ for the domain here.

The qualitative agreement between the structure of this unstable normal mode and the model's storm track is intriguing. However, there are a number of reasons to be cautious about using such a mode as a "theory" for storm tracks. First, in general there will be a spectrum of unstable normal modes, particularly for more complicated

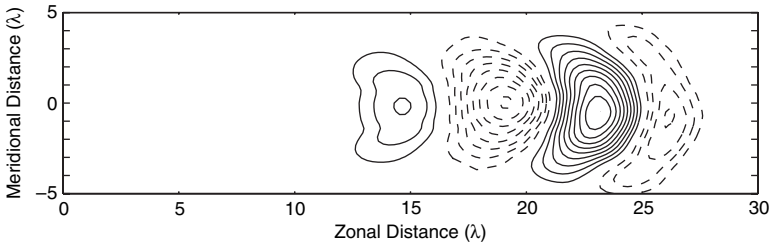

FIGURE 4.9. Upper-layer streamfunction for one phase of the most unstable mode for dynamics linearized about the base-case time-mean flow. Contours are arbitrary, with negative contours dashed and the zero contour omitted.

flows with multiple storm tracks. Unless the growth rate of the most unstable mode is well separated from that of other modes, there is no reason to suspect that the most unstable normal mode should be preferred in such a situation. Secondly, it is now generally believed that in models of this class, as well as in the atmosphere, unstable normal modes are global, rather than local, in character. As discussed at length by Pierrehumbert (1984), this distinction is vital. Local modes have a number of desirable structural properties that in principle make them ideal candidates to explain storm track structures. Their amplitude peaks downstream of the point of maximum baroclinicity of the basic state flow, and decays to zero both downstream and upstream of the peak. Most importantly, local modes do not require a re-entrant domain for their existence. This compact nature ensures that they are not influenced by factors remote from a given localized baroclinic zone. In addition, their growth rate is determined by the growth rate at the point of maximum baroclinicity for a given local baroclinic zone, rather than some domain-averaged measure of baroclinicity.

In contrast, global modes require a re-entrant domain for their existence, and because of this, take very long to become established in any given region. Their growth rate is sensitive not to the peak baroclinicity in the domain, but rather to the baroclinicity averaged throughout the domain. The global modes form a near continuum, and owing to the large time required for a single mode to emerge from random initial conditions, they are physically relevant only insofar as they can be used in combination to represent the evolution of transient wave packets.

For the case here, as well as for the atmosphere, dynamics linearized about the time-mean flow do not support local modes (Lin and Pierrehumbert 1993). Such local modes appear to require rather robust easterlies at the surface to exist, and these are found neither in the model here nor in the atmosphere. In the model here, the lack of local modes may be directly confirmed by inserting a "sponge" well downstream of the storm track that inhibits disturbance recirculation. Doing so eliminates exponentially amplifying disturbances in this particular system.

This leaves us in a quandary—since the most unstable mode is global, there is no reason to expect that this mode in isolation should be more important than other modes with similar, albeit smaller, growth rates. Indeed, the entire question of growth rates is

troublesome, as their link to storm track structure is not immediately obvious—i.e., do larger magnitude linear disturbance growth rates necessarily lead to larger-magnitude storm tracks? The difficulties with the use of unstable normal modes to describe storm tracks may be illustrated by considering the dynamics of the most unstable mode for the sequence of mean flows generated by varying γ. Consistent with the discussion above regarding the dependence of global modes upon the zonally averaged baroclinicity, which as noted in section 4.3 does not vary substantially as a function of γ, there is little variation in the disturbance growth rates with γ. Those growth rates range from an e-folding time of 20 days for $\gamma = 1$ to an e-folding time of 15 days for $\gamma = 5$. The sense of these growth rates is consistent with the changes in bandpass standard deviation as γ is varied, i.e., higher growth rates do correspond to larger bandpass standard deviations. However, this sensitivity of the growth rates is much smaller than it would be if these were local modes (Zurita-Gotor and Chang 2005).

Comparison of the growth-rate variation as a function of γ suggests that normal mode growth must operate over a time scale of 50 days to explain the changes in bandpass standard deviation that occur as γ is varied (cf. Fig. 4.8). This time scale is long compared to the de-correlation time scale for this system, casting doubt on the strict application of normal mode theory as an explanation of storm track behavior for the case here. Further, this result is for inviscid disturbance growth rates; incorporating radiative damping and surface friction neutralizes these normal modes, consistent with the transients driving the time-mean flow to the point of stabilization in a manner similar to a baroclinic adjustment (see chapter 2 in this volume).

While normal-mode analysis does not provide a theory for storm tracks, it provides insight into certain aspects of storm track structure. As outlined above, storm tracks result from the amplification of transient wave packets. This leads to the question of whether such amplification can be understood in terms of linear spatiotemporal growth of wave packets. Assuming a flow is sufficiently zonal, and varies slowly in the streamwise direction, it will support a spectrum of unstable waves. An initially localized disturbance will evolve into a wave packet with time, and it can be shown that the peak of this wave packet will travel at the velocity

$$c_g = \left.\frac{\partial \omega}{\partial k}\right|_{\max \sigma}, \qquad [4.8]$$

where ω denotes the real component of the amplifying disturbance frequency and σ the imaginary component. For a packet developing linearly from an initially localized disturbance, this means the peak of the packet travels at the group speed of the most unstable mode (Swanson and Pierrehumbert 1993). Assuming a baroclinic zone of length L, the quantity $\sigma L/c_g$, i.e., the growth rate multiplied by the time it takes to traverse the baroclinic zone, is the factor by which one expects a given disturbance will amplify as it traverses the baroclinic zone. Larger disturbance growth may occur not only due to rapid growth (σ large), but also for slow propagation (c_g small). Note that

these concepts are based upon disturbance growth in purely zonal flows. This picture appears to capture the amplification of storm track transients as they propagate through the storm track region, as noted by Harnik and Chang (2004). By and large, this is a product of the fact that growth rates for purely zonal flows roughly scale with the shear (Lindzen and Farrell 1980).

In conclusion, normal-mode thinking has its uses in explaining certain details of storm track structure. However, it offers limited information regarding the relative magnitude of storm tracks in response to perturbations in the background mean flow. As such, it is desirable to examine the extent to which other linear approaches might provide a more complete theory for storm tracks.

4.4.2. Stochastic Models

A different approach to the problem of simulating the statistics of storm track transients follows from the work of Farrell and collaborators (Farrell 1984; Farrell and Ioannou 1994). From this perspective, storm track transients are best viewed as stochastically forced disturbances evolving on a baroclinically stable flow. Eddies can still grow on such a flow, for a finite time, through local energy extraction from the background shears. The effects of quadratic nonlinearities are approximated as stochastic excitation plus an augmented dissipation, similar to that done in early studies of homogeneous turbulence, and the governing equations reduce to a multi-dimensional linear Markov process.

This approach has shown certain successes when models linearized about either the observed time-mean flow (Whitaker and Sardeshumkh 1998) or mean flows generated from a general circulation model (GCM) (Zhang and Held 1999) are stochastically forced. For our purposes here, we consider stochastically forced, artificially damped linear dynamics using the base-case time-mean flow of Fig. 4.5, as well as the time-mean flows resulting from the variation of γ as highlighted in Fig. 4.7. The equation solved is (4.7), where the forcing term S'_n includes not only Ekman damping and radiative relaxation, but also stochastic forcing and an artificial Newtonian relaxation of the disturbance potential vorticity fields. The latter two processes are intended to mimic nonlinear wave-wave dynamics, which scatter energy between different wavenumber bands. As noted above, Ekman damping and radiative relaxation of disturbances by itself results in time-mean profiles that are nearly neutral to linear disturbance growth. Hence, there is substantial flexibility in the choice of the level of artificial Newtonian relaxation. Two situations are examined, one with a relaxation time scale of 7 days and the other with a relaxation time scale of 30 days.

The model is forced by independently and randomly exciting the vorticity and temperature components of the quasigeostrophic potential vorticity, following Zhang and Held (1999). By adjusting the relative strength of these two forcings, it is relatively straightforward to tune the stochastic model to reproduce not only the storm track structure but also the transient heat and momentum (or potential vorticity) fluxes.

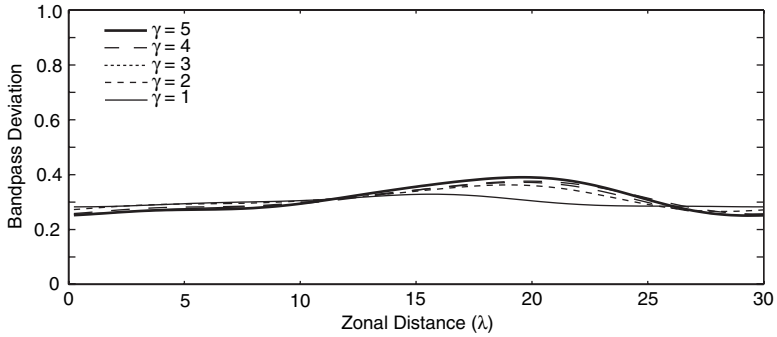

FIGURE 4.10. Stochastically modeled bandpass standard deviation of upper-layer stream function along the channel center for the perturbed storm track cases under the strong damping scenario.

The key question regarding such stochastically forced models concerns what is truly determining the transient statistics. For this, it is useful to define "strong" and "weak" interpretations of stochastic storm track models. The "strong" interpretation follows Whitaker and Sardeshmukh (1998), and is characterized by artificial disturbance relaxation over time scales similar to the de-correlation time scale for storm track systems, roughly one week. Storm track structure and amplitude is then determined primarily by the rapid non-modal growth of disturbances (Farrell 1984). Under this scenario, there is substantial dependence on the manner in which the system is forced, i.e., whether the applied forcing is spatially white in the vorticity, energy, or streamfunction measures. This follows from the work of Farrell and Ioannou (1994), where forcings that have substantial vertical structure preferentially lead to large responses. In contrast, a "weak" interpretation of stochastic storm tracks is marked by relatively weak Newtonian relaxation, exploiting the fact that the action of transients in a model yields a time-mean flow that is quasi-neutral. In this setting, it is natural to expect the dynamics to be much more normal-mode in character, and for the most part insensitive to the structure of the stochastic forcing.

For this simple model, both strong and weak Newtonian relaxation results in adequate reproduction of the storm track structure for the base case shown in Fig. 4.5, as measured, for example, by pattern correlation coefficients. However, as shown in Figs. 4.10 and 4.11, situations with stronger damping (7 days versus 30 days) are quite insensitive to variations in the time-mean flow that occur when γ is varied. As γ increases from 1 to 5, the maximum storm track standard deviation increases only 10% in response to the changes in the flow for the strong relaxation case, and roughly by a factor of 2 for the weak relaxation case. Curiously, Zhang and Held (1999) used relatively large damping in their attempt to explain the midwinter minimum. Their study showed hints of a minimum, but the overall response was much too weak, at least qualitatively resembling the strong damping case shown in Fig. 4.10.

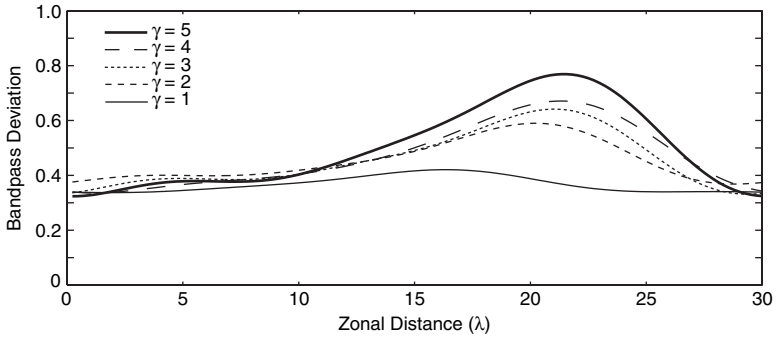

FIGURE 4.11. Stochastically modeled bandpass standard deviation of upper-layer stream function along the channel center for the perturbed storm track cases under the weak damping scenario.

This result highlights some of the unresolved questions regarding the application of stochastically forced storm track models. More experience is necessary to understand the relative roles of forcing structure and disturbance damping before the application of theories of this type can be considered understood. However, the ability of these models to produce statistically steady models of storm track behavior ensures such models will play an important role in furthering our understanding of storm tracks in the future.

4.5. Heuristic Models

While much of what is understood about storm tracks is rooted in linear models, more qualitative models have much to offer as well, with the additional benefit of sharpening the focus on those aspects of storm track dynamics that are truly vital. Over the past decade, it has become increasingly apparent that the fundamental structure in storm track dynamics is not baroclinic growth or conversion per se, but rather the nature and dynamics of the upper-tropospheric waveguide. This is apparent in the paper of Branstator (1995), where changes in transient momentum fluxes are shown to be consistent with the anomalous steering of short wavelength, non-dispersive Rossby waves by anomalous background time-mean flows. Anomalies in transient barotropic vorticity fluxes in the upper troposphere result from the response of transients to changes in that waveguide itself, rather than as some "source" not linked to the large-scale flow that defines that waveguide.

The starting point for any heuristic theory of storm structure is to understand the source of storm track transients. The most promising approach is to note that transient variations in the lower troposphere act primarily to diffuse heat downgradient, with a coefficient of diffusivity equal to the transient streamfunction standard deviation. This is dimensionally consistent, as the streamfunction, like diffusivity, has units of a length multiplied by a velocity, so it provides a simple way to estimate the eddy length and time

scales needed for computing the diffusivity. This point has been made by Kushner and Held (1998) using observed lower-tropospheric winds and heat fluxes.

This heat flux provides a source of transient wave activity (more formally pseudomomentum [see Andrews et al. 1987]) to the upper troposphere. For the upper layer of the two-layer quasigeostrophic system, this wave activity conservation relation has the form

$$\partial_t \mathcal{A}_1 + \frac{\partial}{\partial x}(U_1 \mathcal{A}_1) + \nabla \cdot \mathbf{F} = v_1' \theta', \qquad [4.9]$$

where $\mathcal{A}_1 \equiv \frac{1}{2} q_1'^2 / \partial_y Q_1$ is the pseudomomentum, $\theta' = (\psi_1' - \psi_2')/2$, $\mathbf{F} \equiv [(v_1'^2 - u_1'^2)/2, -u_1' v_1']$ is the two-dimensional Eliassen-Palm flux vector, and Q_1 is the upper-layer zonal-mean potential vorticity distribution. When discussing storm tracks, interest is usually focused on the existence of a zonally oriented upper-tropospheric waveguide. That waveguide will generally be imperfect, with loss of wave activity due to wave breaking in critical layers on the jet flanks, as described, for example, by Killworth and McIntyre (1985), and leakage due to meridional Rossby wave propagation away from the waveguide. These effects are found in the momentum flux $-u_1' v_1'$ in the Eliassen-Palm flux vector **F**. Hence, it is useful to qualitatively rewrite the expression (4.9) as

$$\partial_t \mathcal{A}_1 + \partial_x (c_{gx} \mathcal{A}_1) = v_1' \theta' - \text{breaking} - \text{leakage}, \qquad [4.10]$$

where $c_{gx} = U_1 + (v_1'^2 - u_1'^2)/2$ is the group speed in the zonal direction, and the terms "breaking" and "leakage" incorporate the loss of wave activity in the waveguide.

The development of a heuristic theory of storm track dynamics thus is reduced to two parts: a link between the measure of disturbance amplitude $\mathcal{A}_1$ and the "source" of wave activity $-v_1' \theta'$, and a theory for the breaking and leakage by the waveguide. Regarding the former, Kushner and Held (1998) have shown that to a very good approximation the downgradient heat flux is diffusive, where the diffusivity is simply the transient streamfunction standard deviation. This transient streamfunction standard deviation can be related to the wave activity, providing a closure theory for the baroclinic source. In terms of an upper-layer disturbance streamfunction standard deviation $\langle \psi_1' \rangle = \left(\overline{\psi_1'^2}\right)^{1/2}$, where the bar indicates time-mean, following Kushner and Held (1998) the heat flux will be $\overline{v_1' \theta'} = -\langle \psi_1' \rangle \, \partial_y \overline{\theta} = \langle \psi_1' \rangle \, U_1/2$, provided that the lower-layer winds are small (i.e., the shear is approximately $U_1/2 = -\partial_y \overline{\theta}$ by thermal wind).

With a theory for the source of wave activity in hand, the next challenge is to understand what that wave activity will do when it is in the upper troposphere. The upper troposphere in general will act as a waveguide and reservoir of wave activity, with wave activity within that waveguide being deformed both reversibly and irreversibly. Irreversible wave breaking and/or Rossby wave radiation away from the waveguide will act as sinks of that wave activity. However, for streamwise varying flows, it is the pseudoenergy rather than the pseudomomentum that is the relevant conserved quantity. As shown by Held (1985), these quantities are related by $\mathcal{P} = c\mathcal{A}$, where c is the phase

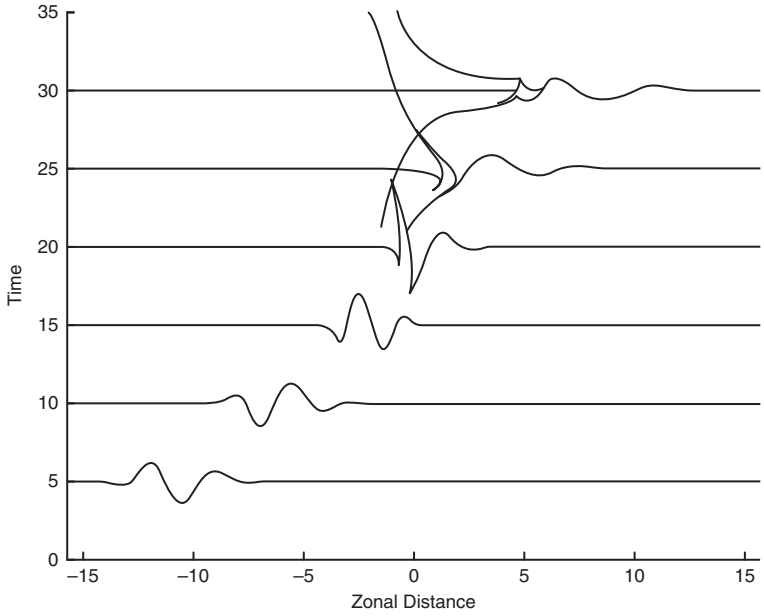

FIGURE 4.12. Loss of disturbance amplitude due to irreversible wave breaking in the simple storm track model of Swanson et al. (1997). The weak flow region is in the center of the domain; disturbances break there first, and their amplitude is reduced after exiting that region. The coordinates are nondimensionalized.

speed of disturbances. In a time-mean setting, wave activity conservation for $\mathcal{P}_1$ then will have the form

$$\partial_x(\overline{c_{gx}\mathcal{P}_1}) = c\left\langle\psi_1'\right\rangle U_1/2 - c(\overline{\text{breaking}} + \overline{\text{leakage}}). \qquad [4.11]$$

Writing $\mathcal{P}_1$ in terms of the disturbance streamfunction ψ_1' closes this equation in the absence of breaking and leakage.

In the absence of leakage or radiation away from the waveguide, wave activity will increase in the waveguide due to the downgradient flux of heat. However, in a re-entrant domain the magnitude of storm track disturbances will be determined by the nature of the leakage and radiation of wave activity away from the waveguide. While theoretical guidance on these effects is limited, the study of Swanson et al. (1997) provides a particularly simple picture. As shown in Fig. 4.12, as disturbances propagate from a region of strong flow into a region of weak flow, their amplitudes are "clipped" due to wave breaking. It is straightforward to show that clipping effectively sets the disturbance amplitude where the flow along the waveguide is weakest. This is similar to the result found in the perturbation experiments of Fig. 4.8; the disturbance standard deviation varies in response to changes in the flow much more in the heart of the storm track than it does in the weak-flow region upstream of the storm track where complicated wave breaking processes occur. Hence, it appears that under certain circumstances regions of weak zonal flow may act as the "gatekeeper" for storm tracks, setting the disturbance

amplitude at the upstream end of the track. Baroclinic growth via downgradient heat fluxes is vital to the structure of storm tracks, but arguably less so for their overall amplitude.

This type of expression suggests why linear techniques are effective at capturing the basic structure of storm tracks, as that structure is primarily determined by the growth of disturbances, which is effectively a linear process. However, the breaking and leakage of disturbances in storm track exit regions is not linear, and nonlinearity may lead to a more substantial decrease in disturbance magnitude than the linear modulation predicted by stochastic theories or normal modes. Perhaps the most important challenge as we move forward in understanding storm track dynamics is to better understand dynamics in storm track exit regions.

4.6. Nonlinear Behavior

Given the ability of linear and quasi-linear theories to explain certain aspects of storm track structure, it may at first glance appear unnecessary to delve too deeply into the role of nonlinearity in storm track dynamics. However, nonlinearity in storm track dynamics has multiple guises. The first guise, that of baroclinically forced turbulence, appears to be adequately captured by the assumptions that turbulent wave-wave interactions can be modeled as an artificially enhanced Newtonian relaxation of disturbances coupled with stochastic forcing of disturbances as noted in section 4.4. However, there is another, less-well discussed aspect of storm track dynamics, namely, whether the global dynamics of storm tracks are robust to changes in the radiative forcing, topography, or damping. In general, it is assumed that there is sufficient "noise" in a storm track system generated by the recirculation of disturbances to maintain robust storm track variability. However, the extent to which this is actually true remains poorly understood, with potentially important ramifications for our understanding of climate variability.

To examine some global properties of storm track systems, consider the base-case forcing of section 4.3, but now varying the supercriticality $\xi = \beta^{-1}$. In all cases, the model is started from an initial condition of radiative equilibrium with small wavy disturbances. For values of $\beta \leq 0.19$, a "normal" climate regime with respect to the observed climate is found similar to that discussed in section 4.2, consisting of a robust storm track displaced downstream from an intense upper-layer jet. The storm track and resultant mean temperature gradient for $\beta = 0.19$ are shown in Fig. 4.13. However, as the supercriticality is further reduced, a bifurcation occurs in the system's dynamics. As shown in Fig. 4.14, decreasing the supercriticality to $\beta = 0.21$ reveals a markedly different climate regime, with a broader, more intense baroclinic zone compared to the "normal" climate found for higher supercriticalities. Transient variability is substantially weaker, with a dipole of transient variability occurring downstream of the jet with standard deviation roughly one-quarter that of the normal climate regime of Fig. 4.13.

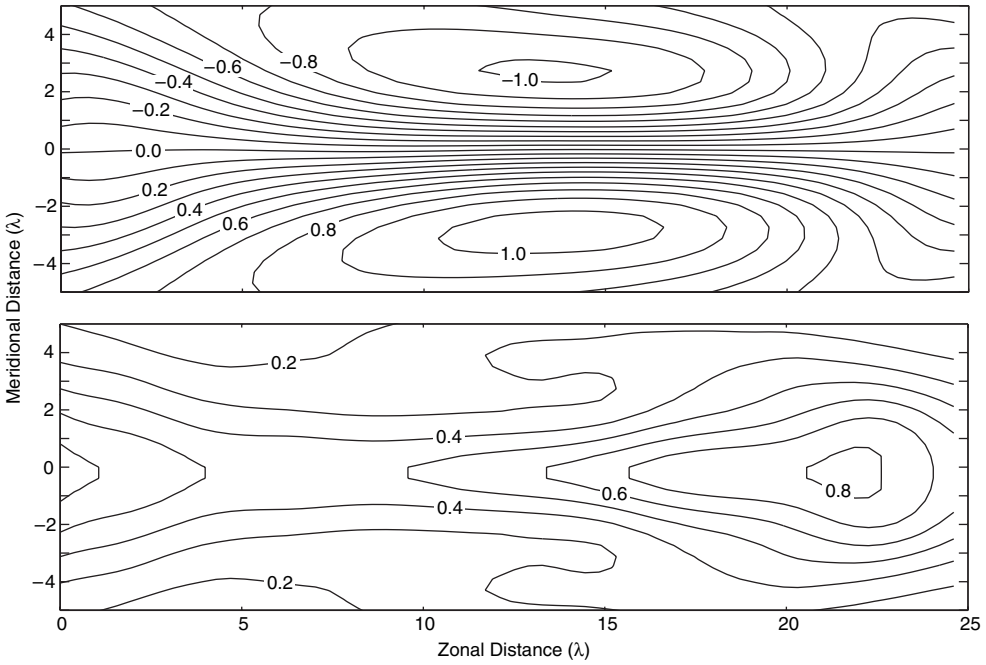

FIGURE 4.13. Top: Time-mean temperature distribution for $\beta = 0.19$ case. Bottom: Total transient standard deviation of upper-layer streamfunction for $\beta = 0.19$ case. Units are λU.

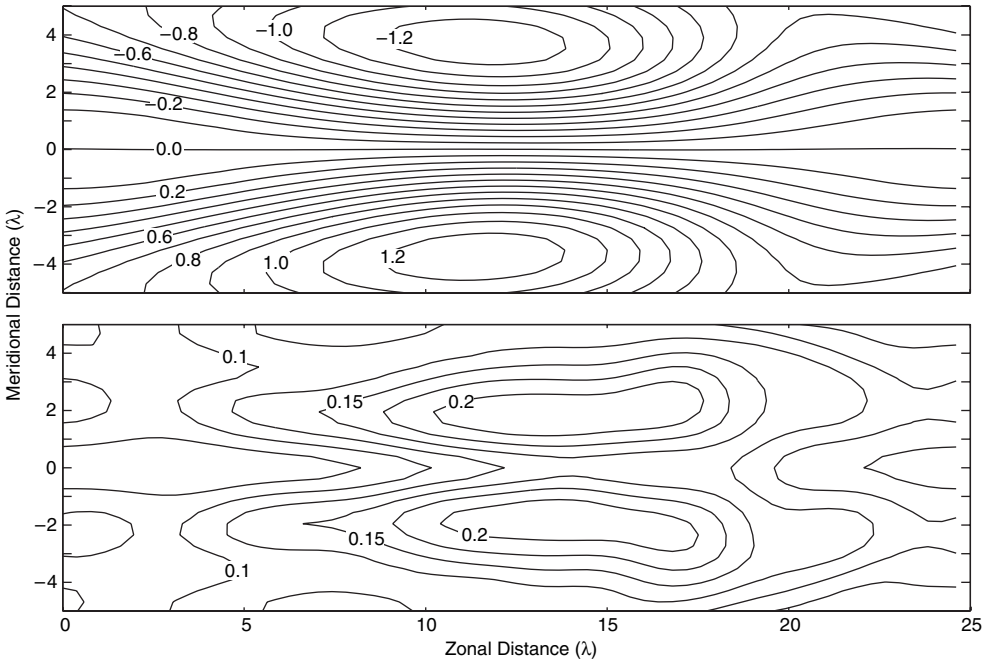

FIGURE 4.14. Top: Time-mean temperature distribution for $\beta = 0.21$ case. Bottom: Total transient standard deviation of upper-layer streamfunction for $\beta = 0.21$ case. Units are λU.

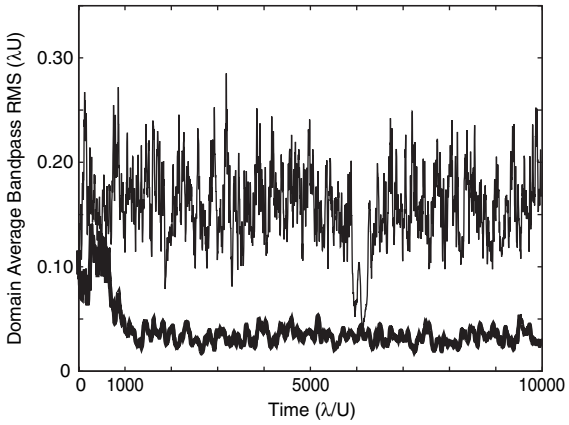

FIGURE 4.15. Time series of domain-averaged bandpass standard deviation of streamfunction variations in simulations started with initial conditions taken from the final state of the $\beta = 0.19$ and $\beta = 0.21$ cases discussed in the text. Both simulations have $\beta = 0.2$.

The variability in this situation is low frequency in character, with the baroclinic zone spawning low-frequency, larger-scale transients on the flanks of the jet. Synoptic scale variability is also present, but mobile transients are substantially weaker in magnitude than for higher supercriticalities.

The traditional method to isolate a bifurcation of this type is to continue solutions from above and below the bifurcation value, making small incremental changes in β, and examine where the jump in dynamical properties occur. Following this procedure, it is found that over the parameter range $\beta \in (0.19, 0.21)$, multiple climates occur in this storm track system for different initial conditions. For example, consider two model simulations with the model supercriticality fixed at $\beta = 0.2$, with initial conditions respectively taken from the respective final state of the simulation with $\beta = 0.19$ of Fig. 4.13 and the simulation with $\beta = 0.21$ of Fig. 4.14. Other than the initial condition, the simulations are identical. Figure 4.15 shows the time series of the domain-averaged bandpass standard deviation (time scales less than 10 days) for the two simulations resulting from these initial conditions. After a period of some transient adjustment, the two simulations maintain very different levels of synoptic transient variability for what appear to be arbitrarily long times.

It appears that for this particular forcing this idealized storm track system possesses a hysteresis, insofar as the model's system state depends upon where the initial condition was taken, whether above or below the bifurcation point. Further, since these solutions are separately chaotic and irregular, it appears as if the system also possesses two coexisting strange attractors, each with quite different climates. While multiple attractors in simple atmospheric models have been noted in a number of different contexts, the presence of baroclinic instability is generally assumed to eliminate such behavior, leading instead to regime-like behavior in the underlying dynamics.

Complicated behavior associated with these two attractors is found for this storm track system—sensitive dependence of the ultimate climate upon initial conditions and "bursts" of synoptic transient activity that appear and disappear suddenly are part of this system's phenomenology.

One must of course take results arising from a model without full dynamical complexity with a grain of salt. However, the presence of this type of behavior does raise a question not often asked in our current examination of climate dynamics: is climate unique? If this type of behavior is found in more complete models, it would open the possibility of strong climate changes in response to rather innocuous triggers, as well as threshold-type behavior, all mediated by storm track dynamics. Significantly, such behavior does appear in the paleoclimate record, in the apparent sensitivity of the hemispheric and even global atmosphere to forcing localized in the North Atlantic basin arising from alterations to the thermohaline circulation in the paleoclimate record (see Dansgaard et al. 1989 and chapter 12 in this volume).

4.7. Conclusions

Where do we stand with understanding storm tracks? The best current theoretical models of storm track dynamics suggest that storm tracks may be adequately modeled as the response of linear dynamics to incoherent stochastic forcing, with baroclinic development of certain preferred disturbances giving the storm tracks their unique character. However, in reality the "forcing" in such stochastic linear storm track models is the result of internal nonlinear dynamics, and there is no reason that such forcing need to be simple or consistent given changes to either external parameters or in response to internal variations in the large-scale flow. The effects of this can be as subtle as a stochastic model's inability to capture changes in storm track amplitude due to an altered basic-state flow, or as profound as the multiple strange attractor behavior shown in section 4.6.

The fundamentally nonlinear transient response to deformation at the downstream end of baroclinic zones emerges as a problem of particular importance, as the ability of transients to transit this zone appears to provide a limit on storm track amplitudes for the entire system. Unfortunately, theoretical guidance of the physics governing how disturbances evolve through such diffluent flow environments is extremely limited. Much more remains to be discovered about storm track dynamics in this region before our understanding of even current-day storm track fluctuations can be considered complete.

Above all, intermediate models still have a role to play in furthering our understanding of storm track dynamics, and hence the climate system. There are always many choices that must be made in the study of storm track dynamics. Is it better to fully explore the parameter space of an intermediate model, or apply that computer power

toward simulations with a more complete model? Is it better to test theories completely on storm track models of the same complexity as the theory itself, or attempt to use them to explain variations in the observed storm tracks? While these are questions that have no easy answers, the state of understanding storm tracks may well be better served by inquiries along the lines of the first part of each question. There is still much work that remains in studying the dynamics of storm tracks before their role in the climate can be considered understood.

References

Andrews D.G. (1984). On the stability of forced non-zonal flows. *Q. J. Roy. Met. Soc.,* **110,** 657–662.

Andrews D.G., Holton J.R., and Leovy C.B. (1987). *Middle Atmosphere Dynamics.* Academic Press, 489 pages.

Blackmon M.L. (1976). A climatological spectral study of the 500 mb geopotential height of the Northern Hemisphere. *J. Atmos. Sci.,* **55,** 1607–1623.

Blackmon M.L., Wallace J.M., Lau N.-C., and Mullen S.L. (1977). An observational study of the Northern Hemisphere wintertime circulation. *J. Atmos. Sci.,* **34,** 1040–1053.

Branstator G. (1992). The maintenance of low-frequency atmospheric anomalies. *J. Atmos. Sci.,* **49,** 1924–1945.

Branstator G. (1995). Organization of storm track anomalies by recurring low-frequency circulation anomalies. *J. Atmos. Sci.,* **52,** 207–226.

Broecker W.S. (1997). Thermohaline circulation, the Achilles Heel of our climate system: Will man-made CO_2 upset the balance? *Science,* **278,** 1582–1588.

Cai M. and Mak M. (1990). Symbiotic relation between planetary waves and synoptic scale waves. *J. Atmos. Sci.,* **47,** 2953–2968.

Chang E.K.M. (1993). Downstream development of baroclinic waves as inferred from regression analysis. *J. Atmos. Sci.,* **50,** 2038–2053.

Chang E.K.M. (1999). Characteristics of wave packets in the upper troposphere. Part II: Hemispheric and seasonal differences. *J. Atmos. Sci.,* **56,** 1729–1747.

Chang E.K.M. (2000). Wave packets and life cycles of troughs in the upper troposphere: Examples from the Southern Hemisphere summer season of 1984/85. *Mon. Wea. Rev.,* **128,** 25–50.

Chang E.K.M. (2001).The structure of baroclinic wave packets. *J. Atmos. Sci.,* **58,** 1694–1713.

Chang E.K.M. and Orlanski I. (1993). On the dynamics of a storm track. *J. Atmos. Sci.,* **50**, 999–1015.

Chang E.K.M., Lee S., and Swanson K. (2002). Storm track dynamics. *J. Climate,* **15,** 2163–2183.

Dansgaard W. et al. (1989). The abrupt termination of the Younger Dryas climate event. *Nature,* **339,** 532–534.

Farrell B.F. (1984). Modal and non-modal baroclinic waves. *J. Atmos. Sci.,* **41,** 668–673.

Farrell B.F. and Ioannou P. (1994). A theory for the statistical equilibrium energy and heat flux produced by transient baroclinic waves. *J. Atmos. Sci.,* **51,** 2685–2698.

Fredricksen J.S. (1983). Disturbances and eddy fluxes in Northern Hemisphere flows: Instability of three-dimensional January and July flows. *J. Atmos. Sci.,* **40,** 836–855.

Frisius T., Lunkeit F., Fraedrich K., and James I. (1998). Storm-track organization and variability in a simplified atmospheric global circulation model. *Q. J. Roy. Met. Soc.,* **124,** 1019–1044.

Hall N.M.J., Hoskins B.J., Valdes P.J., and Senior C.A. (1994). Storm tracks in a high-resolution GCM with doubled carbon dioxide. *Q. J. Roy. Met. Soc.,* **120,** 1209–1230.

Harnik N. and Chang E.K.M. (2004). The effects of variations in jet width on the growth of baroclinic waves: Implications for midwinter Pacific storm track variability. *J. Atmos. Sci.,* **61,** 23–40.

Held I.M. (1985). Pseudomomentum and the orthogonality of modes in shear flows. *J. Atmos. Sci.,* **42,** 2280–2288.

Held I.M. and Hoskins B.J. (1985). Large-scale eddies and the general circulation of the troposphere. *Adv. Geophysics,* **28A,** 3–31.

Held I.M., Ting M., and Wang H. (2002). Northern winter stationary waves: Theory and modeling. *J. Climate,* **15,** 2125–2144.

Hoskins B.J. and Hodges K.I. (2002). New perspectives on the Northern Hemisphere winter storm tracks. *J. Atmos. Sci.,* **59,** 1041–1061.

Killworth P.D. and McIntyre M.E. (1985). Do Rossby-wave critical layers absorb, reflect or over-reflect? *J. Fluid Mech.,* **161,** 449–492.

Kushner P.J. and Held I.M. (1998). A test, using atmospheric data, of a method for estimating oceanic eddy diffusivity. *Geophys. Res. Lett.,* **25(22),** 4213–4216.

Kushner P.J. and Held I.M. (1999). Potential vorticity fluxes and wave-mean flow interaction. *J. Atmos. Sci.,* **56,** 948–958.

Lau N.-C. and Holopainen E.O. (1984). Transient eddy forcing of the time-mean flow as identified by geopotential tendencies. *J. Atmos. Sci.,* **41,** 313–328.

Lee S. (1995). Localized storm tracks in the absence of local instability. *J. Atmos. Sci.,* **52,** 977–989.

Lee S. and Held I.M. (1993). Baroclinic wave packets in models and observations. *J. Atmos. Sci.,* **50,** 1413–1428.

Lim G.H. and Wallace M. (1991). Structure and evolution of baroclinic waves as inferred from regression analysis. *J. Atmos. Sci.,* **48,** 1718–1732.

Lin S.-J. and Pierrehumbert R.T. (1993). Is the midlatitude flow absolutely unstable? *J. Atmos. Sci.,* **50,** 505–517.

Lindzen R.S. and Farrell B.F. (1980). A simple approximate result for the maximum growth rate of baroclinic instabilities. *J. Atmos. Sci.,* **37,** 1648–1654.

Nakamura H. (1992). Midwinter suppression of baroclinic wave activity in the Pacific. *J. Atmos. Sci.,* **49,** 1629–1642.

Pierrehumbert R.T. (1984). Baroclinic instability. *J. Atmos. Sci.,* **41,** 2141–2162.

Pierrehumbert R.T. and Swanson K.L. (1995). Baroclinic instability. *Ann. Rev. Fluid Mech.,* **27,** 419–467.

Simmons A.J. and Hoskins B.J. (1980). Barotropic influences on the growth and decay of nonlinear baroclinic waves. *J. Atmos. Sci.,* **36,** 1239–1254.

Swanson K.L., Kushner P.J., and Held I.M. (1997). Lower-tropospheric heat transport in the Pacific storm track. *J. Atmos. Sci.,* **54,** 1533–1543.

Swanson K.L. and Pierrehumbert R.T (1993). Nonlinear baroclinic wave packet evolution on a baroclinically unstable jet. *J. Atmos. Sci.,* **51,** 384–396.

Whitaker J.S. and Sardeshmukh P.D. (1998). A linear theory of extratropical synoptic eddy statistics. *J. Atmos. Sci.,* **55,** 237–258.

Zhang Y. and Held I.M. (1999). A linear stochastic model of a GCM's midlatitude storm tracks. *J. Atmos. Sci.,* **56,** 3416–3435.

Zurita-Gotor P. and Chang E.K.M. (2005). The impact of zonal propagation and seeding on the eddy-mean flow equilibrium of a zonally varying two-layer model. *J. Atmos. Sci.,* **62,** 2261–2273.